ASTRONOMY & ASTROPHYSICS
SUPPLEMENT SERIES

Astron. Astrophys. Suppl. Ser. **133**, 249–255 (1998)

Photoionization cross sections for Fe XVIII

D. Donnelly, K.L. Bell, and F.P. Keenan

School of Mathematics and Physics, The Queen's University of Belfast, Belfast, BT7 1NN, Northern Ireland

Received March 10; accepted June 3, 1998

Abstract. A sophisticated R-matrix calculation is performed for the photoionization of the fine-structure levels of the ground state of Fe XVIII. High resolution total and partial cross sections are obtained with the later restricted to the cases of the Fe XVIII ion being left in one of the fine-structure levels corresponding to the energetically lowest 11 LS states of Fe XIX after ionization. Both sets of cross sections are obtained using the Breit-Pauli R-matrix approximation which allows for the possibility of fine structure splitting in both resonances and thresholds. We find extensive resonance structure in the 99 to 113 Ryd photon energy range, a high percentage of which arises from 2p photoionization leaving the ion in the $2s^2 2p^4\ ^3P_2$ state while the background cross section is constructed almost exclusively of 2p and 2s photoionization with the former dominant in both photoionization cases. Relativistic effects are found to be important in obtaining accurate threshold positions as well as being responsible for a significant drop in the background cross section in comparison with various calculations done in LS coupling. We believe that this is the first relativistic calculation for this ion.

Key words: atomic data — atomic processes

1. Introduction

X-ray emitting plasmas are a phenomenon frequently encountered in astrophysical studies, and are characteristic of various accretion-powered sources such as X-ray binaries, cataclysmic variables and active galactic nuclei (Mushotzky et al. 1993; Kahn & Liedahl 1995). In addition, X-rays are detected from the high temperature plasmas which constitute the upper transition regions and coronae of the Sun and other stars (Phillips et al. 1982). X-rays emitted from these phenomena are the result of many different atomic processes occurring within the plasma, such as electron impact excitation and photoabsorption, both of which frequently involve ions of iron at various stages of excitation. Modelling of the X-ray emission of each of the above sources thus requires detailed atomic data about the various processes which occur within the associated plasma.

Unfortunately, while electron impact of various ions of iron has been studied in sufficient detail, photoionization still lacks serious consideration. Some previous work has been performed, such as that by Verner et al. (1993) and Verner & Yakovlev (1995), but even these are lacking inner shell photoionization data explicitly on Fe XVIII. In addition, recent observations by the Advanced Satellite for Cosmology and Astrophysics (ASCA) have shown that the current atomic data are inadequate for a proper quantitative analysis of plasma emission (Fabian et al. 1994; Liedahl et al. 1995). The Opacity Project team have calculated total photoionization cross sections for the ions of iron using the R-matrix codes, and have included their results in the TOPBASE database (Seaton et al. 1992; Cunto & Mendoza 1992) for use by the astrophysical community. These calculations represent a significant improvement over the data of Verner et al. due to their consideration of the possibility of the existence of resonance structure. However, these R-matrix calculations included only 6 target states without the introduction of electron correlation effects; were performed using an LS-coupling approximation; and the partial cross sections resulting from leaving the iron ion in one of the target states after photoionization have not been extracted from the total cross section.

Each of the ions of iron has a particular significance in astrophysics. Specifically, Fe XVIII has been linked (Liedahl et al. 1990, 1992) with an emission feature at about 16 Å found in low mass X-ray binaries (Vrtilek et al. 1991). Investigation of the atomic processes involving this ion is thus desirable. Electron impact excitation of Fe XVIII has already been studied using the R-matrix method by Mohan et al. (1987). In this paper, we

Send offprint requests to: K.L. Bell (kl.bell@qub.ac.uk)

therefore investigate the L-shell photoionization of Fe XVIII using the R-matrix method to obtain both total and partial photoionization cross sections.

2. Method

We employ the Breit-Pauli R-matrix method (Scott & Burke 1980) to calculate the photoionization cross sections. This method has the advantage of including the effects of resonances which converge onto the LSJ target states of Fe XIX which are included in the calculation. The present work is based on including in the eigenfunction expansion the following 11 Fe XIX LS target states, Φ_i: $2s^22p^4\ ^3P$, $2s^22p^4\ ^1D$, $2s^22p^4\ ^1S$, $2s2p^5\ ^3P^\circ$, $2s2p^5\ ^1P^\circ$, $2p^6\ ^1S$, $2s^22p^33s\ ^3S^\circ$, $2s^22p^33s\ ^3P^\circ$, $2s^22p^33s\ ^3D^\circ$, $2s^22p^33s\ ^1D^\circ$ and $2s^22p^33s\ ^1P^\circ$. Each of these target states are represented by configuration interaction wavefunctions of the form

$$\Phi\left(LS\right) = \sum_{n=1}^{M} a_n \phi_n \left(\alpha_n LS\right) \tag{1}$$

where ϕ_n $n = 1, ..., M$ represents a set of configuration state functions which possess the same total $LS\pi$ symmetry and are constructed from a set of one-electron orbitals whose radial part is given by a linear combination of Slater-type orbitals

$$P_{nl}\left(r\right) = \sum_{j=1}^{k} c_{jnl} \left[\frac{\left(2\zeta_{jnl}\right)^{2I_{jnl}+1}}{\left(2I_{jnl}\right)!}\right]^{\frac{1}{2}} r^{I_{jnl}} \mathrm{e}^{-\zeta_{jnl}r}. \tag{2}$$

The configuration state functions are chosen to be those configurations generated by considering the addition of one electron from the orbital set {1s, 2s, 2p, 3s, 3p, 3d} to the basis distributions $2s^22p^3$, $2s2p^4$ and $2p^5$. A total of 68 configurations were thus considered in representing the target states. The 1s, 2s and 2p orbitals used in the representation of these wavefunctions were taken to be the Hartree-Fock orbitals of the ground state of Fe XIX determined by Clementi & Roetti (1974) while the remaining orbitals were generated by the configuration interaction code CIV3 (Hibbert 1975) in the following manner. Treating I_{jnl} as fixed, the c_{jnl} and ζ_{jnl} parameters of Eq. (2) are then treated as variational parameters. The 3s orbital was thus obtained by varying these parameters in order to minimize the energy of the $2s^22p^3(^4S)3s\ ^3S^\circ$ state. Similarly the 3p and 3d orbitals were optimized using the energies of the $2s^22p^3(^4S)3p\ ^3P$ and $2s^22p^3(^4S)3d\ ^3D^\circ$ states respectively where in each case only a single configuration was used in the wavefunction expansion. The resulting parameters for these orbitals are given in Table 1.

The energies obtained for these target states were calculated in LS-coupling using the CIV3 configuration interaction code and in LSJ-coupling using the RECUPD module of the R-matrix codes where the same orbitals and level of correlation were used in each case. The results

Table 1. Radial function parameters for oxygen-like Fe XIX orbitals

Function	c_{jnl}	I_{jnl}	ζ_{jnl}
3s	0.24937	1	18.84274
	−1.44272	2	7.81808
	1.91095	3	6.82215
3p	0.66177	2	10.46492
	−1.22624	3	6.25767
3d	0.01186	3	12.14146
	0.99146	3	6.52229

of both calculations are presented in Table 2 and compared with the experimental results tabulated by Corliss & Sugar (1982) and the relativistic calculations of Dasgupta (1995) (using the non-relativistic operators plus the spin-orbit operator, mass correction operator and the Darwin term). (Note that a comparison between the LS calculation and the data of Corliss & Sugar requires consideration of a weighted average of the ground state provided by Corliss & Sugar). Clearly some discrepancy exists between the LS-coupling calculation and the previous studies. However, attempts at introducing further correlation into this calculation had minimal effects on these energies. Threshold positions and thus resonance positions in general would have been of insufficient accuracy if a solely LS-coupling calculation had been performed. Thus, it is clearly essential to include relativistic effects, in that the introduction of interaction between different $LS\pi$ symmetries is highly relevant to the accuracy of the target state energies. The results of the LSJ-coupling calculation are highly satisfactory and examination of the eigenvectors verifies that significant mixing between different $LS\pi$ symmetries possessing the same $J\pi$ value does indeed occur particularly in the ground state terms. (For example in the LS calculation the ground state, ^3P, is reasonably pure but in the relativistic calculation 11% of the $^3P_2$ ground state is made up of the $2s^22p^4\ ^1D_2$ configuration. This is enough to lower the ground state by as much as 8 a.u.).

The $(N+1)$-electron wavefunction, Ψ is expanded in the following manner

$$\Psi = \sum_k A_{Ek} \psi_k \tag{3}$$

where A_{Ek} are energy dependent coefficients and ψ_k are states which form a basis for the total wavefunction, are energy independent and are given by the expansion

$$\begin{aligned}\psi_k\left(x_1, ..., x_{N+1}\right) = \\ \mathcal{A}\sum_{ij} c_{ijk}\overline{\Phi}_i\left(x_1, ..., x_N; \hat{\mathbf{r}}_{N+1}\sigma_{N+1}\right)\frac{1}{r_{N+1}}u_{ij}\left(r_{N+1}\right) \\ + \sum_j d_{jk}\chi_j\left(x_1, ..., x_{N+1}\right)\end{aligned} \tag{4}$$

where $\overline{\Phi}_i$ are the channel functions obtained by coupling the target states Φ_i with the angular and spin functions of

Table 2. Target state energies (in a.u.) relative to the ground state of Fe XIX. Previous data are from the tabulation by Corliss & Sugar (1982) and from the relativistic calculation of Dasgupta (1995)

Number	Target state	Present LS calculation	J-value	Present Relativistic calculation	Corliss & Sugar	Dasgupta
1			2	0.000000	0.000000	0.0000
2	$2s^2 2p^4\ ^3P$	0.000000	0	0.331780	0.343073	
3			1	0.396415	0.407395	
4	$2s^2 2p^4\ ^1D$	0.469237	2	0.779794	0.769441	
5	$2s^2 2p^4\ ^1S$	1.021499	0	1.469373	1.481344	
6			2	4.222184	4.204424	
7	$2s2p^5\ ^3P^\circ$	3.743038	1	4.503292	4.486392	
8			0	4.704507	4.692275	
9	$2s2p^5\ ^1P^\circ$	5.116381	1	5.831343	5.774917	
10	$2p^6\ ^1S$	8.738452	0	9.830549	9.722747	
11	$2s^2 2p^3 3s\ ^3S^\circ$	30.416669	1	30.605849	30.436268	30.4720
12			2	31.027342	30.923795	30.9300
13	$2s^2 2p^3 3s\ ^3D^\circ$	30.914906	1	31.077168	30.928352	30.9355
14			3	31.224804	31.065042	31.0785
15	$2s^2 2p^3 3s\ ^1D^\circ$	31.051822	2	31.314511	31.137943	31.1635
16			0	31.572245	31.470555	31.5170
17	$2s^2 2p^3 3s\ ^3P^\circ$	31.246286	1	31.609108	31.543456	31.5510
18			2	31.808179	31.757603	31.8065
19	$2s^2 2p^3 3s\ ^1P^\circ$	31.383815	1	31.931847	31.825948	31.8765

the continuum electron, u_{ij}, to form states of total angular momentum and parity. $\mathcal{A}$ is the antisymmetrization operator which accounts for electron exchange between the target electrons and the free electron while χ_i represents the quadratically integrable (L^2) functions (or $(N+1)$-electron configurations) which are formed from the bound orbitals and are included to ensure completeness of the total wavefunction. These configurations are generated by the addition of two electrons from the orbital basis set into the basis distributions $2s^2 2p^3$, $2s2p^4$ and $2p^5$. This approach ensures that a measure of equilibrium is attained between the target and $(N+1)$-electron systems by treating the Fe XVIII states as bound states of the (Fe XIX + e^-) system. Since we are interested in photoionization of both the Fe XVIII ground state ($2s^2 2p^5\ ^2P^\circ_{\frac{3}{2}}$) and the first excited state $2s^2 2p^5\ ^2P^\circ_{\frac{1}{2}}$) the following $J\pi$ symmetry transitions interest us: ${\frac{3}{2}}^\circ \rightarrow {\frac{1}{2}}^e, {\frac{3}{2}}^e, {\frac{5}{2}}^e$ and ${\frac{1}{2}}^\circ \rightarrow {\frac{1}{2}}^e, {\frac{3}{2}}^e$. The entire range of LS matrices which contribute to the above $J\pi$ symmetries are included in the calculation and are recoupled in the manner of Scott & Burke (1980) to give the ${\frac{3}{2}}^\circ$, ${\frac{1}{2}}^\circ$, ${\frac{1}{2}}^e$, ${\frac{3}{2}}^e$ and ${\frac{5}{2}}^e$ Hamiltonian matrices.

Using an R-matrix radius of 2.2 a.u., 25 continuum orbitals for each value of $l \leq 6$ and a free electron energy mesh of $1\ 10^{-3}$ Ryd, the R-matrix codes (Berrington et al. 1987; Seaton 1987) are then utilized to calculate the photoionization cross sections. The ionization energy of the Fe XVIII ground state was found to be 99.954 Ryd, in excellent agreement with the experimental value of 100.108 ± 0.294 Ryd tabulated by Corliss & Sugar (1982). The $2s^2 2p^5\ ^2P^\circ_{\frac{1}{2}}$ Fe XVIII bound state was found to be at 0.96068 Ryd relative to the ground state, compared with the value 0.93541 Ryd given by Corliss & Sugar (a difference of only 2.6%), suggesting that the approach used in the calculation of bound states is of sufficient accuracy.

3. Results and discussion

Using the mathematical model thus far described the total photoionization cross sections are calculated for both the ground state, $2s^2 2p^5\ ^2P^\circ_{\frac{3}{2}}$, and first excited state, $2s^2 2p^5\ ^2P^\circ_{\frac{1}{2}}$, of Fe XVIII and the results are presented in Fig. 1

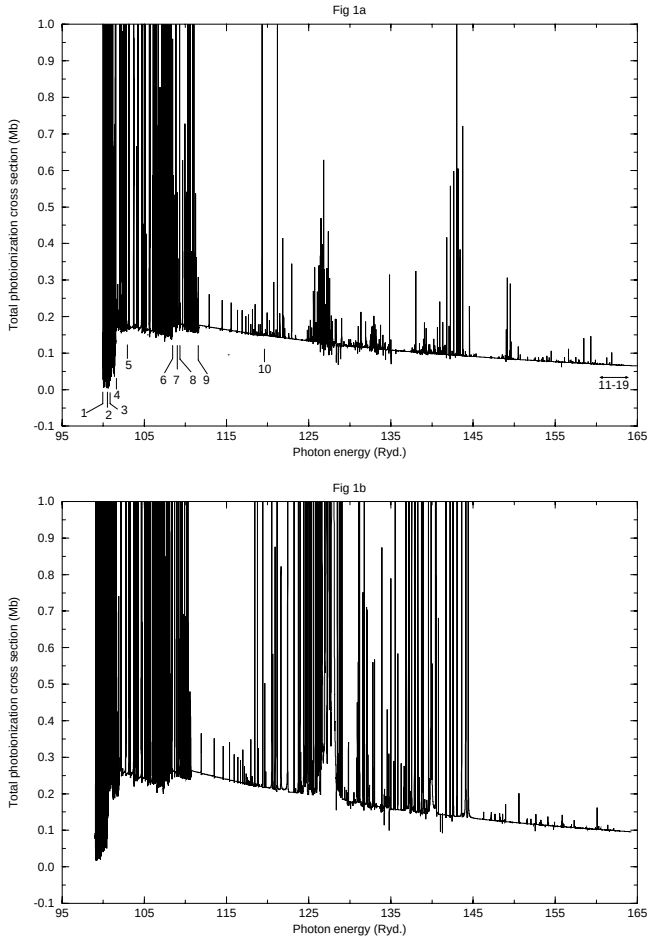

Fig. 1. Total photoionization cross sections for the photoionization of Fe XVIII in the 95 to 165 Ryd photon energy range: **a)** photoionization of the ground state, $2s^2 2p^5\ ^2P_{\frac{3}{2}}$. Threshold are marked using Table 2 as a reference, **b)** photoionization of the first excited state, $2s^2 2p^5\ ^2P_{\frac{1}{2}}$

along with threshold positions. In order to compare with the only previous calculation, namely the Opacity Project data obtained for the photoionization of the LS-coupled $2s^2 2p^5\ ^2P^\circ$ ground state (Butler & Zeippen, unpublished), a weighted average of the present cross sections for photoionization from the $2s^2 2p^4\ ^2P^\circ_{\frac{3}{2}}$ and $^2P^\circ_{\frac{1}{2}}$ levels was obtained. Comparison is made in Fig. 2 and we note that the value of the ionization energy obtained by Butler & Zeippen is too low, and so for comparison purposes their data has been shifted in energy by 3.55 Ryd. The agreement in the background cross section between the Opacity project data and the weighted average data is within 30%. This difference observed in the background is due to the inclusion of relativistic effects which would seem to be supported by the positive effect such effects had on the target state energies and by an LS R-matrix calculation which uses the present approximation but omits all relativistic

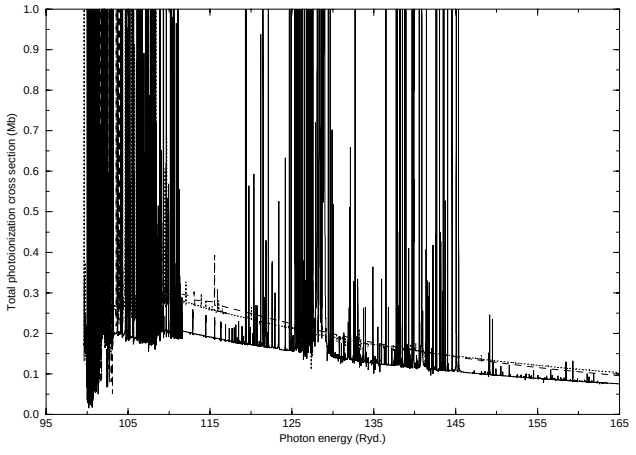

Fig. 2. Weighted average of the total photoionization cross sections for the photoionization of the ground state, $2s^2 2p^5\ ^2P_{\frac{3}{2}}$ and first excited state, $2s^2 2p^5\ ^2P_{\frac{1}{2}}$, of Fe XVIII (solid curve) compared with the Opacity project data (dashed curve) and the present calculation performed in LS coupling (dotted curve), in the 95 to 165 Ryd photon energy range

effects (a smaller resolution of 1 10^{-2} Ryd. is used in this case). The results of this calculation are also plotted in Fig. 2 and comparision of these results with the Opacity project data demonstrates an agreement within 5%. Due to the same target states being used in both these calculations up to a photon energy of 160 Ryd we conclude that this drop in the background corresponds to the introduction of correlation in the target. Consequently the further drop in the background observed in the LSJ calculation is due to the significant increase in the CI introduced into the target state wavefunctions through the spin orbit operator.

The present calculations demonstrate a general shape of the photoabsorption spectrum that is in excellent accord with the Opacity project data with the exception that the present work resolves a single shape resonance at 128 Ryd. Examination of Fig. 1 shows that this is a result of photoionization of the $\frac{1}{2}^\circ$ state only. Figures 1 and 2 illustrate extensive resonance structure in the 99 to 113 Ryd photon energy range. Figure 3 thus presents a more detailed examination of this range with the full height of the resolved resonances presented. We note the excellent agreement in the resonance positions compared with those present in the Opacity project spectrum. However, numerous additional resonances have been resolved in the present work while other resonances have a larger magnitude. Both phenomena are due to the increased sophistication of the target state representation and the different resolution used in the two calculations.

Partial photoionization cross sections (for both photoionization cases) corresponding to the residual Fe XIX

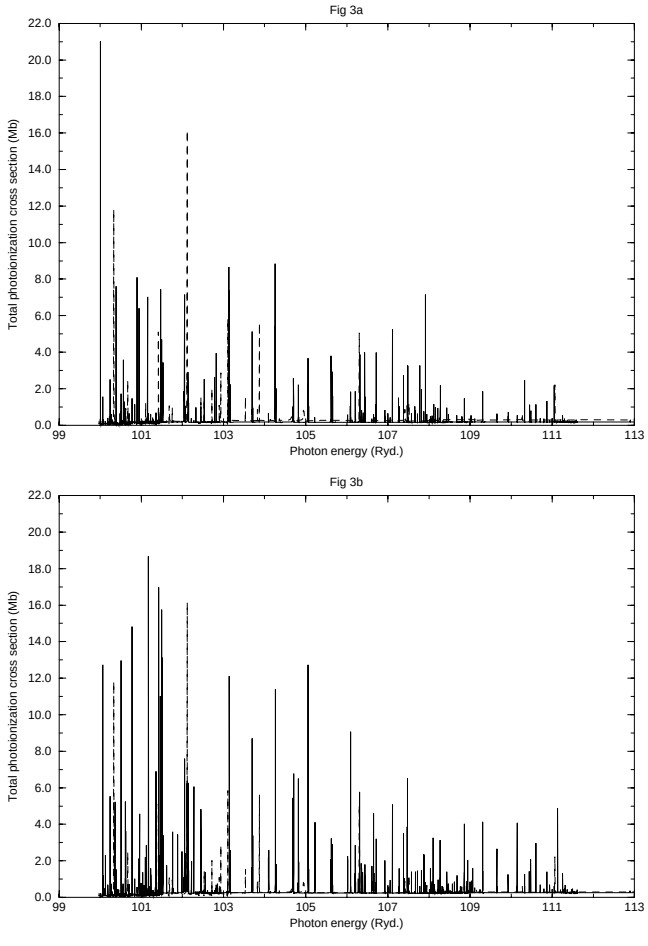

Fig. 3. Total photoionization cross sections for the photoionization of Fe XVIII (solid curve) compared with the Opacity project data (dashed curve) in the 99 to 113 Ryd. photon energy range: **a)** photoionization of the ground state, $2s^2 2p^5\ ^2P_{\frac{3}{2}}$, **b)** photoionization of the first excited state, $2s^2 2p^5\ ^2P_{\frac{1}{2}}$

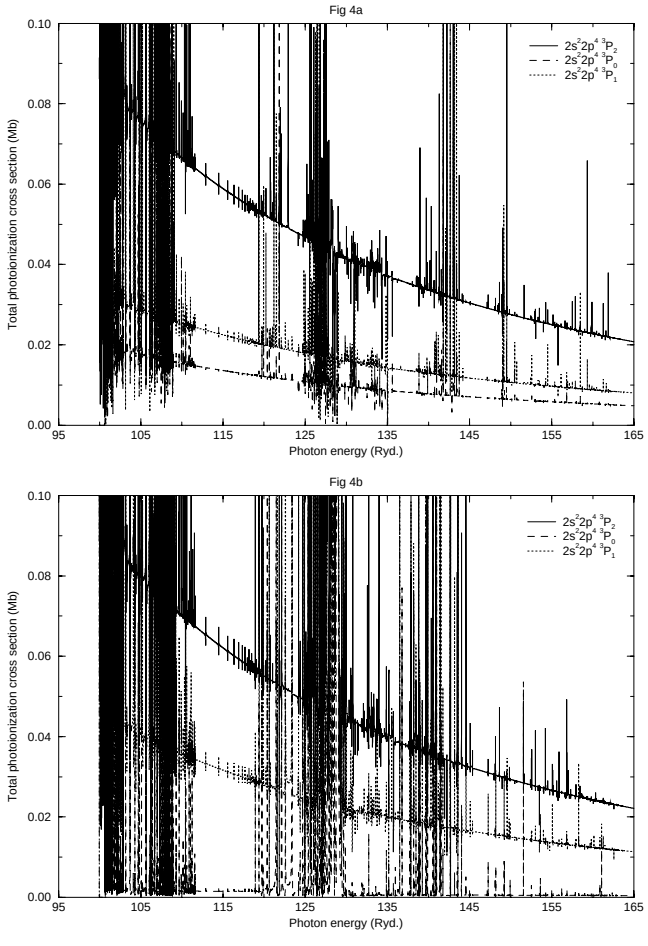

Fig. 4. Partial photoionization cross sections resulting from 2p photoionization of the ground state and first excited state of Fe XVIII where the residual ion is left in the $2s^2 2p^4\ ^3P_{2,1,0}$ states: **a)** photoionization of the ground state, $2s^2 2p^5\ ^2P_{\frac{3}{2}}$, **b)** photoionization of the first excited state, $2s^2 2p^5\ ^2P_{\frac{1}{2}}$

ion being left in one of the fine-structure levels corresponding to the 6 energetically lowest LS target states are presented in Figs. 4 to 7. Photoionization of the Fe XVIII ground state is clearly dominated by the mechanism which leaves Fe XIX in its ground state with the contribution of this process to the total cross section being more than double that of any other photoionization mechanism. We note that all the partial cross sections corresponding to 2p photoionization leaving the Fe XIX ion in the $2s^2 2p^4$ states make significant contributions to the total cross section as do those corresponding to 2s photoionization resulting in $2s2p^5$. However, of these two possiblities the one involving 2p photoionization is clearly the dominant process while the effect that double electron excitation of 2s or 2p (resulting in $2p^6$ and $2s^2 2p^3 3s$ respectively) has in this energy range is negligible. Partial cross sections for these target states have thus been omitted except for those of the $2p^6\ ^1S_0$ cross section which exhibit a small amount of resonance structure. In general partial cross sections for photoionization from the $\frac{1}{2}^\circ$ state follow the same pattern as those from the ground state with the exception that the mechanism resulting in the residual ion existing in the Fe XIX $2s^2 2p^4\ ^1D_2$ state now dominates despite the partial cross sections for the Fe XIX ground state being of the same magnitude as in the ground state photoionization case. Thus $2p$ photoionization makes up a much higher percentage of $2s^2 2p^5\ ^2P^\circ_{\frac{1}{2}}$ photoionization than in the ground state case and is responsible for the greater magnitude of the background cross section of the former compared with the latter.

The extensive resonance structure in the 99 to 113 Ryd photon energy range is due primarily to photoionization of Fe XVIII resulting in the $2s^2 2p^4\ ^3P_2$ state in *both* the photoionization of $J = \frac{3}{2}$ and $J = \frac{1}{2}$ cases.

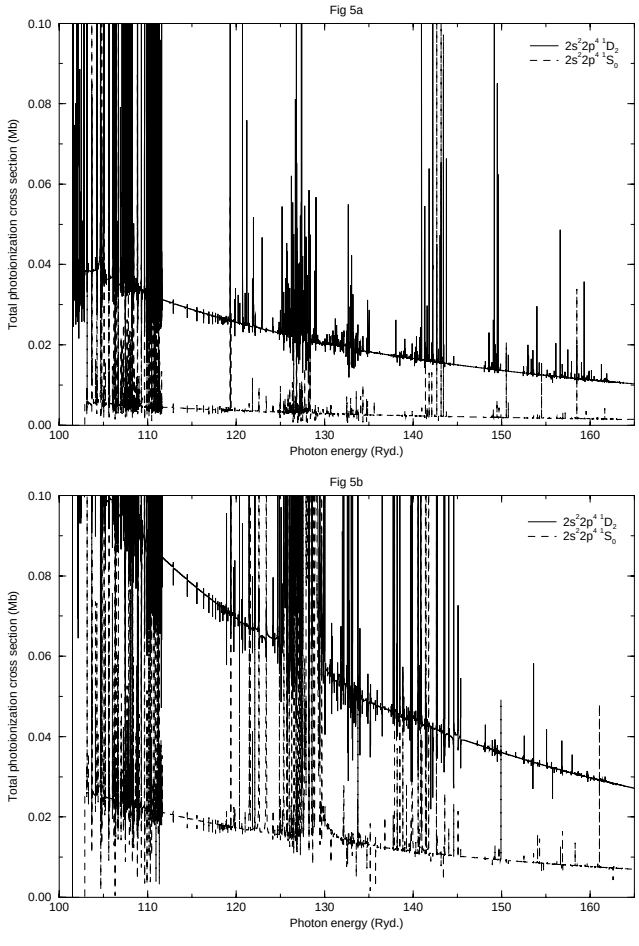

Fig. 5. Partial photoionization cross sections resulting from 2p photoionization of the ground state and first excited state of Fe XVIII where the residual ion is left in the $2s^2 2p^4\ ^1D_2$ and $^1S_0$ states: **a)** photoionization of the ground state, $2s^2 2p^5\ ^2P_{\frac{3}{2}}$, **b)** photoionization of the first excited state, $2s^2 2p^5\ ^2P_{\frac{1}{2}}$

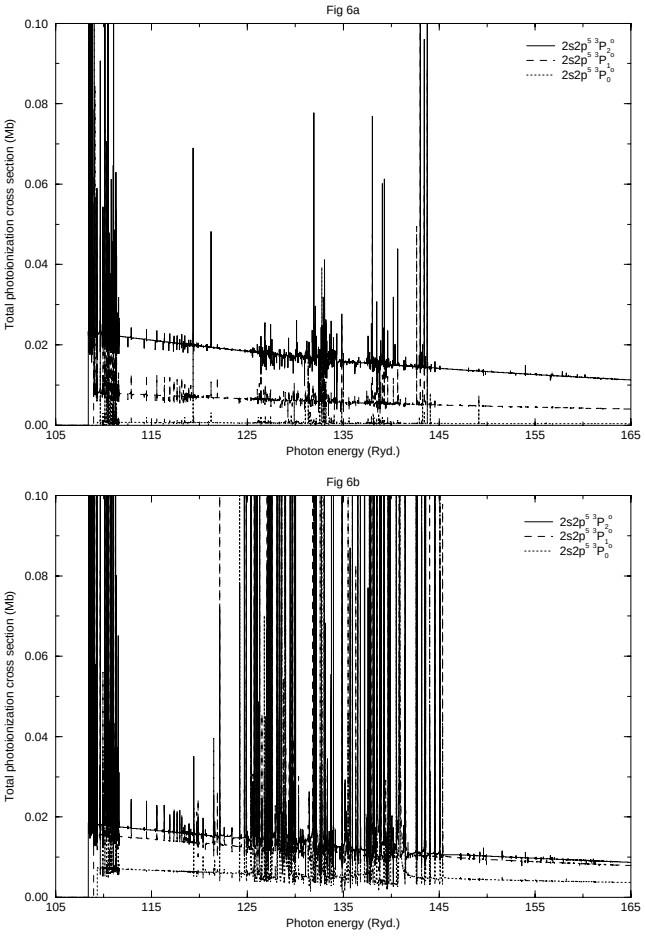

Fig. 6. Partial photoionization cross sections resulting from 2s photoionization of the ground state and first excited state of Fe XVIII where the residual ion is left in the $2s2p^5\ ^3P^\circ_{2,1,0}$ states: **a)** photoionization of the ground state, $2s^2 2p^5\ ^2P_{\frac{3}{2}}$, **b)** photoionization of the first excited state, $2s^2 2p^5\ ^2P_{\frac{1}{2}}$

The photoionization spectrum of the first excited state also demonstrates resonance structure in the 125 to 130 photon energy range where a shape resonance is also apparent. Both features are due primarily to 2p photoionization but no individual partial cross sections dominate these structures. (Figures which illustrate the full height of the resonances in the energy range required for each partial cross section were used in the development of these conclusions. It was not felt worthwhile to include these in the present publication. However partial cross sections to *all 19* target levels listed in Table 2 for both photoionization calculations are available from the authors on request).

4. Summary

In summary we have presented the most complete calculation of both total and partial photoionization cross sections for Fe XVIII yet available. We note the favorable comparison with previous work. However, a much greater resolution and target state representation as well as the inclusion of fine structure effects results in a lower background as well as a substantially greater resolution of resonance structure. Finally we note that the calculations presented within this publication are a clear indication of the need for the inclusion of relativistic effects in calculations concerning highly ionized iron.

Acknowledgements. DD would like to thank PPARC for financial support. All R-matrix calculations were performed on the CRAY J932 located at the Rutherford Appleton Laboratory.

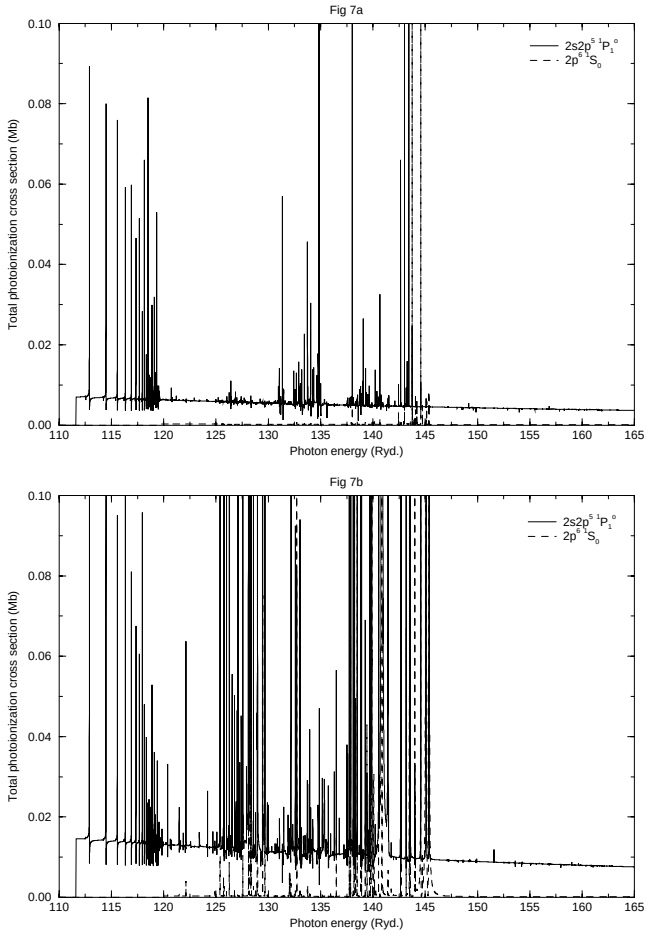

Fig. 7. Partial photoionization cross sections resulting from 2s photoionization of the ground state and first excited state of Fe XVIII where the residual ion is left in the $2s2p^5\ ^1P_1$ and $2p^6\ ^1S_0$ states: **a)** photoionization of the ground state, $2s^22p^5\ ^2P_{\frac{3}{2}}$, **b)** photoionization of the first excited state, $2s^22p^5\ ^2P_{\frac{1}{2}}$

References

Berrington K.A., Burke P.G., Butler K., et al., 1987, J. Phys. B: At. Mol. Phys. 20, 6379

Clementi E., Roetti C., 1974, At. Data Nucl. Data Tab. 14, 177

Corliss C., Sugar J., 1982, J. Phys. Chem. Ref. Data 11, 135

Cunto W., Mendoza C., 1992, Rev. Mexicana Astron. Astrofis. 23, 107

Dasgupta A., 1995, ApJS 101, 401

Fabian A.C., Arnaud K.A., Bautz M.W., Tawara, Y., 1994, ApJ 436, L63

Hibbert A., 1975, Comput. Phys. Commun. 9, 141

Kahn S.M., Liedahl D.A., 1995, Physics with Multiply Charged Ions, Liesen D. (ed.). Plenum Press, New York, p. 169

Liedahl D.A., Kahn S.M., Osterheld A.L., Goldstein W.H., 1990, ApJ 350, L37

Liedahl D.A., Kahn S.M., Osterheld A.L., Goldstein W.H., 1992, ApJ 391, 306

Liedahl D.A., Osterheld A.L., Goldstein W.H., 1995, ApJ 438, L115

Mohan M., Baluja K.L., Hibbert A., Berrington K.A., 1987, J. Phys. B: At. Mol. Phys. 20, 6319

Mushotzky R.F., Done C., Pounds K.A., 1993, ARA&A 31, 717

Phillips K.J.H., Leibacher J.W., Wolfson C.J., et al., 1982, ApJ 256, 774

Scott N.S., Burke P.G., 1980, J. Phys. B: At. Mol. Phys. 13, 4299

Seaton M.J., 1987, J. Phys. B: At. Mol. Phys. 20, 6363

Seaton M.J., Zeippen C.J., Tully J.A., et al., 1992, Rev. Mexicana Astron. Astrofis. 23, 19

Verner D.A., Yakovlev D.G., Band I.M., Trzhaskovskaya M.B., 1993, At. Data Nucl. Data Tab. 55, 233

Verner D.A., Yakovlev D.G., 1995, A&AS 109, 125

Vrtilek S.D., McClintock J.E., Seward F.D., Kahn S.M., Wargelin B.J., 1991, ApJS 76, 1127